



Nanosecond laser ablation processes in aluminum-doped zinc-oxide for photovoltaic devices

D. Canteli^{a,*}, S. Fernandez^a, C. Molpeceres^b, I. Torres^a, J.J. Gandía^a

^a División de Energías Renovables, Energía Solar Fotovoltaica, CIEMAT, Avda. Complutense, 22, 28040 Madrid, Spain

^b Centro Láser, Universidad Politécnica de Madrid, Ctra. de Valencia Km 7.3, 28031 Madrid, Spain

ARTICLE INFO

Article history:

Available online 21 October 2011

Keywords:

Laser processing
Aluminum zinc oxide

ABSTRACT

Aiming to a future use in thin film solar modules, the processing of aluminum doped zinc oxide thin films with good optoelectronic properties with a nanosecond-pulsed ultraviolet laser has been studied. The ablation threshold fluence of the films has been determined and associated with the material properties. The ablation process has been optimized and grooves with good properties for photovoltaic devices have been obtained. The morphology of the ablated surfaces has been observed by confocal microscopy and its structure has been characterized by Raman spectroscopy. The influence of ablation parameters like focus distance, pulse energy and repetition frequency in the groove morphology has been studied with special attention to the thermal effects on the material structure.

© 2011 Elsevier B.V. All rights reserved.

1. Introduction

Aluminum-doped zinc oxide (AZO) and its use as a transparent conductive oxide (TCO) have received great attention in recent years [1,2,5–7]. Besides mandatory properties such as high visible transparency in the visible wavelength range and a high electrical conductivity, its chemical stability, non-toxicity and the low cost and abundance of its components in the nature make AZO a very interesting and promising TCO material. Several techniques have been used to deposit AZO thin films but most of them need high temperature processes to obtain low resistivity values. Radio frequency (RF) magnetron sputtering allows the deposition of AZO at low temperatures, down to room temperature (RT), with good morphological, mechanical and optoelectronic properties at high deposition rates [1].

Due to the properties of thin film cells and to the need of reducing fabrication costs, thin film solar modules production is based on the monolithic interconnection of the solar cells. The process to form the electrical union between adjoined cells includes three laser steps that are integrated into the fabrication process. Each of these steps electrically isolates zones of the various films forming the cell structure, allowing the connection (monolithic union), as follows: TCO cutting, a-Si:H ablation, and back contact removal. This work deals with the first of these steps, used to pattern the front TCO contact to electrically isolate the different cells [2,3].

The quality of the monolithic union strongly affects the final properties of the whole module. Several methods have been used to perform the monolithic union, like mechanical scribing, photolithography or masking wires. In recent years laser scribing is being considered a very appropriate tool, because of its selectivity and the possibility to obtain high quality grooves [4]. This evidences the need to study the laser processes involved in module production since defects generated during the scribing process have terrible effects on solar-panel operation. Typical issues found in poorly optimized laser scribes in a-Si:H devices include flake generation at the scribe edges, presence of debris in the surrounding area and laser-induced thermal effects. All of them generally result in irreversible damages to the finished product that can even cause the complete failure of the solar panel and must be minimized.

In the ablation processes the selection of the laser wavelength results of main importance. AZO is a degenerated semiconductor with a direct band gap. It has the lower states of the conduction band occupied by free electrons, which increases very much its conductivity. If the incident laser light energy is smaller than the optical band gap (E_g) of the material the energy is mostly absorbed by electrons inside a band and is transferred to the lattice on a picosecond timescale. Much of the energy absorbed goes to the lattice of the material, heating it. On the other hand, if the laser light energy is greater than E_g , the absorbed energy is used to promote electrons from the valence band to the conduction band and less energy is used to heat the lattice. If the laser light used has energy similar to the material E_g most of this energy is spent in the ablation process, minimizing thermal effects. AZO films reported bandgap range from 3.2 to 3.7 eV, varying with the film properties [1,5]. Taking this

* Corresponding author. Tel.: +34 91 346 60 39.

E-mail address: david.canteli@ciemat.es (D. Canteli).

Table 1
Main properties of the samples used in this work.

Sample	Deposition T ($^{\circ}\text{C}$)	Thickness (nm)	Resistivity ρ ($\Omega\text{ cm}$)	T_{average} (%) 400–800 nm
A	25	740	3.0×10^{-3}	70.6
B	100	500	1.1×10^{-3}	80.8
C	250	430	3.8×10^{-4}	85.0
D	300	325	7.8×10^{-4}	84.6

into account, 355 nm laser light, with energy of 3.49 eV, seems an adequate tool for the ablation processes.

The main aim of this paper is to study the interaction between 355 nm laser light with AZO thin films deposited by RF magnetron sputtering. For that purpose, AZO films have been deposited at different temperatures, and the ablation threshold, i.e. the minimum energy density needed to start the ablation over the material surface, have been measured and related to the films optical properties. In order to achieve grooves with optimal characteristics for application in PV devices a study of the influence of the main process parameters was carried out. Pulse energy, repetition frequency and spot profile have been related to the effects over the groove morphology, and the thermal effects on the material structure have been evaluated.

2. Materials and methods

2.1. Sample preparation

AZO thin films were deposited on $10\text{ cm} \times 10\text{ cm}$ Corning glass 7059 in a commercial MVSsystems magnetron sputtering operating by RF power. The ceramic target ($\text{ZnO}:\text{Al}_2\text{O}_3$, 98%:2%wt) had a purity of 99.995% and a density of 6.6 g/cm^3 . The target to substrate distance was kept at 84 mm and the base pressure and working pressure were $2.7 \times 10^{-5}\text{ Pa}$ and 0.7 Pa, respectively. The sputtering RF power was fixed at 60 W and the temperatures of deposition used in this study were room temperature (RT) (sample A), 100°C (sample B), 250°C (sample C) and 300°C (sample D). More details of this process can be found in Ref. [1].

2.2. Laser source

The laser used in this work was a diode-pumped solid-state laser ($\text{Nd}:\text{YVO}_4$) from Spectra Physics with a fundamental frequency of 1064 nm that can be doubled (532 nm) or tripled (355 nm) using modules. An electro-mechanical shutter allows the operation with a repetition frequency within 15–300 kHz with pulse duration of about 13 ns. In this study only light with 355 nm and an average power of 5 W at a repetition frequency of 50 kHz was used. The laser beam was led and focused on the sample surface by an optical system including two mirrors, a beam expander that can change the spot size, a digital scanner (HurryScan II 14, Scanlab) and a lens with 250 mm focal. This allowed an operation zone of $150\text{ mm} \times 150\text{ mm}$ with a scanning speed of 11 mm/s to 10 m/s. The beam profile was measured using a beam analyzer. An almost Gaussian shape, with a little distortion in one of the directions (fitting of 92% and 85% to a Gaussian function in the X, Y axis) was observed. A Gaussian beam profile was assumed in all the calculations performed in this work.

2.3. Material characterization

The optical transmittance and reflectance of the AZO films were measured with a Perkin–Elmer Lambda 1050 UV/Visible/NIR spectrophotometer. The absorption coefficient was obtained from the transmittance spectra using a numerical method based in nonlinear programming models [6].

For morphological characterization of the grooves an optical microscopy (Olympus PMG3, Olympus SZ–CTV) and a confocal laser scanning microscopy (Leica DCM 3D) were used. Raman spectra were measured using a commercial InVia Renishaw Raman spectrometer employing the 514.5 nm line of an Ar laser.

The measurement of the laser spot size and of the ablation threshold was based in the fluence (energy per unit surface) profile $\Phi(r)$ of the Gaussian laser pulse [7,8]. The pulse fluence has a radial distribution characterized by Eq. (1), where $\Phi_0 = 2E_p/\pi w_0^2$ is the fluence maximum, located at the centre of the pulse, E_p is the pulse energy, r is the radius from the pulse centre, and w_0 is the radius where the fluence value drops to $1/e^2$ of Φ_0 .

$$\Phi(r) = \Phi_0 \exp\left(\frac{-2r^2}{w_0^2}\right) \quad (1)$$

From this equation a relation between the square of the crater diameter D made by a laser pulse with the fluence was obtained (Eq. (2)):

$$D^2 = 2w_0^2 \ln\left(\frac{\Phi_0}{\Phi_{th}}\right) \quad (2)$$

where Φ_{th} is the ablation threshold fluence, defined as the minimum laser fluence required for start the material ablation.

By plotting D^2 versus the natural logarithm of the pulse energy the laser spot size can be obtained and the maximum fluence of the laser pulse calculated. With this, the ablation threshold can be determined from the relation between the D^2 and the natural logarithm of Φ_0 .

To calculate the total fluence received by the material surface during a laser process a numerical addition of the fluence of consecutive pulses at the centre of the groove was made, using Eq. (1) for the pulse fluence.

3. Results and discussion

3.1. AZO films properties

The AZO films used in this study showed good optoelectronic properties. Table 1 shows the main properties of each sample. Its average transparency in the range of 400–800 nm varied from 70% to 85%, and its electrical resistivity varied from 7.8×10^4 to $3 \times 10^3\ \Omega\text{ cm}$. Because of the conditions of deposition, the thickness of each sample was different, and not homogeneous in the entire glass surface. The value given in Table 1 is the maximum thickness, in the central area of the glass, where optical measurements were made.

Fig. 1 shows the absorption coefficient for each of the samples obtained from the transmittance spectra. Focusing in the laser wavelength, 355 nm, the values for the absorption coefficient ranged from $1.5 \times 10^4\text{ cm}^{-1}$ for the less absorbent film to $3.5 \times 10^4\text{ cm}^{-1}$.

The ablation threshold of the samples was measured as explained before. Fig. 2a shows the relation between the square of the crater diameter D^2 versus the natural logarithm of the maximum fluence of the laser pulse for each sample. The extrapolation of D^2 to zero yields Φ_{th} . Fig. 2b shows the relation between the ablation threshold fluence as a function of the absorption

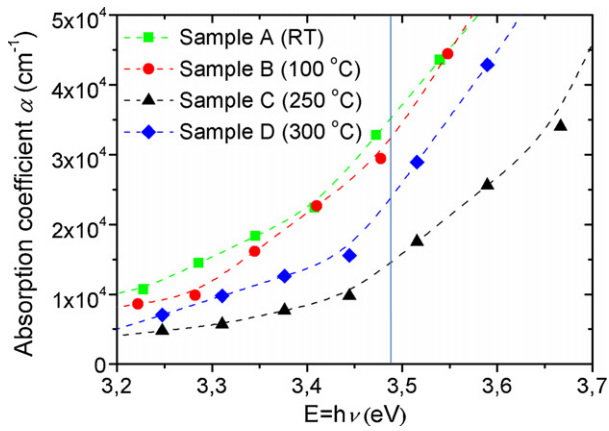


Fig. 1. Absorption coefficient of the AZO films, obtained from the transmittance spectra. The values at the laser wavelength 355 nm (3.49 eV), are pointed out.

coefficient at the laser wavelength. As the absorption coefficient of the film increased, the ablation threshold decreased from 0.47 J/cm^2 to 0.23 J/cm^2 . That is, as the film has a stronger absorption a lower density of energy is needed to begin to damage the material.

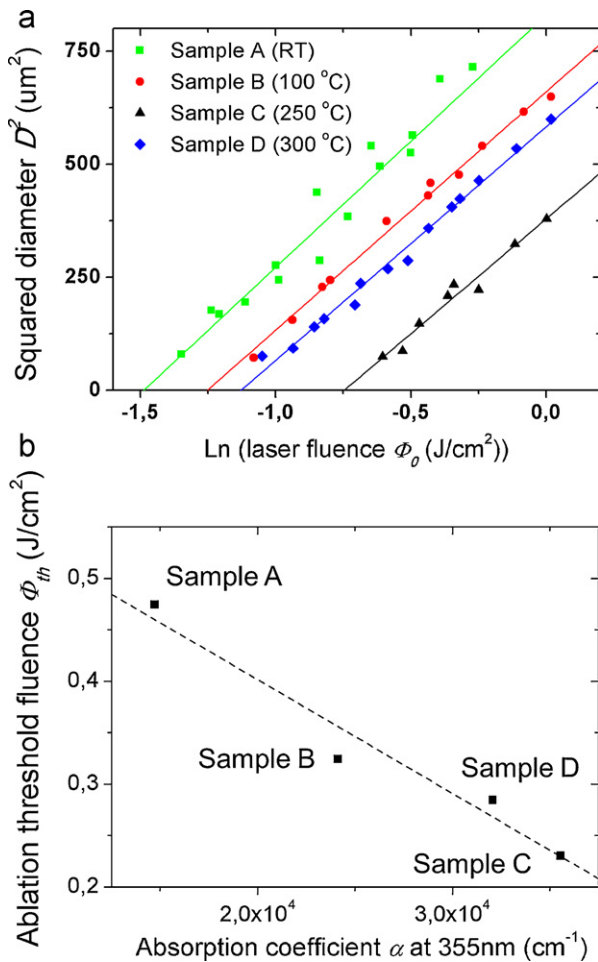


Fig. 2. (a) Square of the crater diameter D^2 versus the natural logarithm of the maximum fluence of the laser pulse Φ_0 . The extrapolation of D^2 to zero makes the calculus of Φ_{th} possible. (b) Ablation threshold fluence versus the absorption coefficient of AZO films at 355 nm (laser wavelength).

3.2. Groove characterization

Since the ultimate objective is for these grooves to be used in thin film PV devices it is necessary that the scribes performed have a clean aspect, with no ridges on the edges and a flat bottom without substrate damage. To obtain grooves with optimal characteristics, laser processes were performed on samples at different distances from laser beam focus, at different repetition frequencies (from 15 to 150 kHz) with E_p from $3.5 \times 10^{-7} \text{ J}$ to $1.4 \times 10^{-5} \text{ J}$ and processing speeds v from 10 to 120 mm/s. To avoid effects of the thickness in the groove characteristics, tests were made in regions with similar thickness for all the samples about 400 nm.

Initial experiments were performed with the sample positioned in the focus plane. It is worth mentioning that the same following behaviour was observed in all of the samples tested, regardless of the deposition temperature used.

By varying E_p , the effect of the laser fluence was investigated. The results showed that working at too high fluence the substrate was damaged whereas an incomplete ablation of the AZO films was observed when the fluence was too low. In addition, it was also observed that some of the material was melted and pushed over the groove sides, where it solidified resulting in ridges and spikes. The height of these ridges vary with the process parameters, specially with the total fluence and the repetition frequency, and ranges from less than 100 nm to several microns. Fig. 3 shows confocal images and profiles of grooves made in focus position using a high (Fig. 3a) and a low (Fig. 3b) repetition frequencies and slightly out of focus using low repetition frequency (Fig. 3c). These images are from the sample A, but the same behaviour was observed in all the samples. Larger ridges were observed working at high repetition frequencies. As a general behaviour, working at fluences of about $10\text{--}15 \text{ J/cm}^2$ decreases the lateral ridges height, being these smaller for low repetition frequencies. Since these ridges can cause shortening of the device structure they must be minimized. Working slightly out of focus led to a wider laser beam radius and hence a lower Φ_0 value for the same value of E_p . In this position at low frequency (20 kHz) and using a total fluence of about $10\text{--}15 \text{ J/cm}^2$ clean, complete grooves were obtained for all the samples. The obtained grooves had much better morphologic characteristics: almost no melted material was observed and the ridges in the groove edges did not appear. Grooves had smooth walls and a relative flat bottom, and no debris or residues in the AZO surface were observed. On the other hand, cracks in the surface at the groove edge appeared. These cracks were present in all the samples. Although of small size, they will be a source of weakening of the material, or of shunts between the films deposited in later steps. A preliminar study by Raman spectroscopy has been made to determine any changes in the film structure, but the optimal use of these processes must be checked in final devices.

3.3. Raman spectroscopy

Grooves made at low repetition frequency (20 kHz) with the AZO samples positioned slightly out of focus were studied by Raman spectroscopy to analyze the effect of laser ablation in their structures, especially in the surrounding areas of the grooves that showed little cracks.

Raman spectra taken on the samples deposited at different temperatures showed structure differences. Fig. 4 shows the Raman spectra of the four samples. Due to the thickness of the samples (less than a micron) the signal of the substrate is visible in all cases.

The sample deposited at higher temperature showed two intense peaks at ~ 270 and $\sim 580 \text{ cm}^{-1}$. The peak at $\sim 270 \text{ cm}^{-1}$ belonged to the scattering due to the B2 silent mode and 580 with a LO mode [9]. A less intense peak was observed at $\sim 370 \text{ cm}^{-1}$, corresponding to A1TO modes, and two weak peaks at $\sim 440 \text{ cm}^{-1}$ (E2

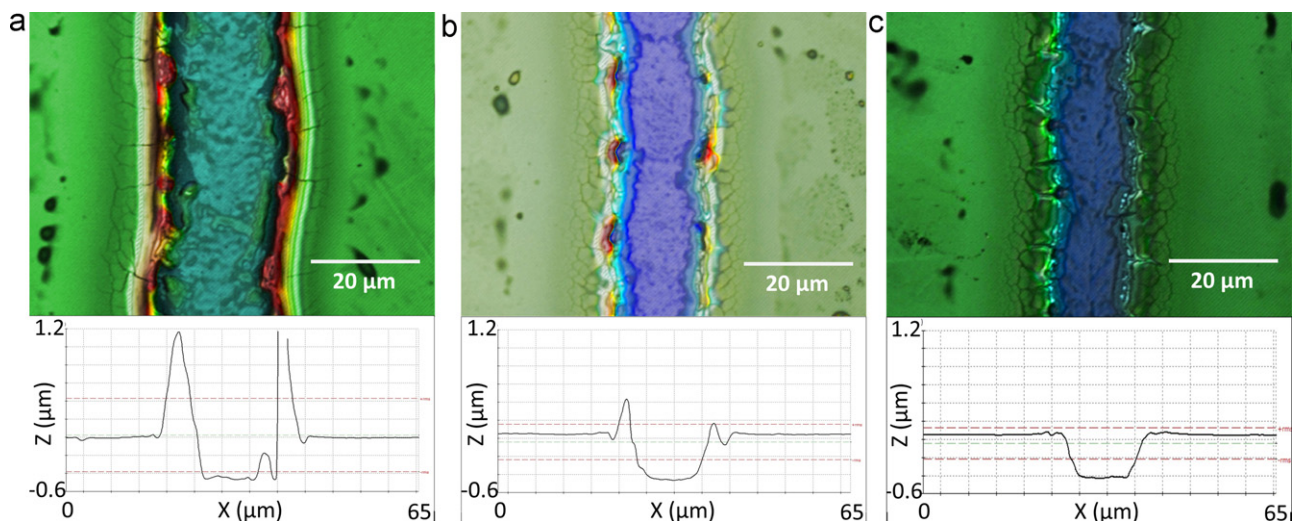


Fig. 3. Confocal microscopy images and profiles of grooves made with similar fluence (about $10\text{--}15\text{ J/cm}^2$ at the groove centre) over the sample A. The same behaviour was observed in the either samples. (a) At focus position with high repetition frequency ($>50\text{ kHz}$). (b) At focus position with low repetition frequency (20 kHz). (c) Out of focus at low repetition frequency (20 kHz). Working in focus, ridges and peaks were observed on the edges of the groove. Meanwhile, working at low repetition frequencies slightly out of focus no peaks appeared.

mode) and $\sim 510\text{ cm}^{-1}$, corresponding to modes highly localized near the grain boundaries. These bands were characteristics of AZO thin films [9,10].

As the deposition temperature was lower the Raman spectra changed. A wide band centred at $\sim 565\text{ cm}^{-1}$ and ranging from 530 to 590 cm^{-1} appeared, with an asymmetry at lower energies. The asymmetry of the band at low energies has been observed previously by Tzolov et al. [9] and is associated to the coupling of LO phonon-plasmon modes (PPM). The broadening of this band and the appearance of another broad band from 100 to 250 cm^{-1} is under study. The peak at $\sim 510\text{ cm}^{-1}$ showed a slightly increased intensity meanwhile the B2 silent mode ($\sim 270\text{ cm}^{-1}$) was less intense and the E2 and A1TO modes disappeared.

The main differences appear between samples A and C, deposited at RT and 250°C . To study the influence of the ablation various spectra were taken on these samples, at points located at the groove centre, at the groove edge and at four and eight microns far from the groove edge. Also a spectrum was taken at the non-treated sample surface.

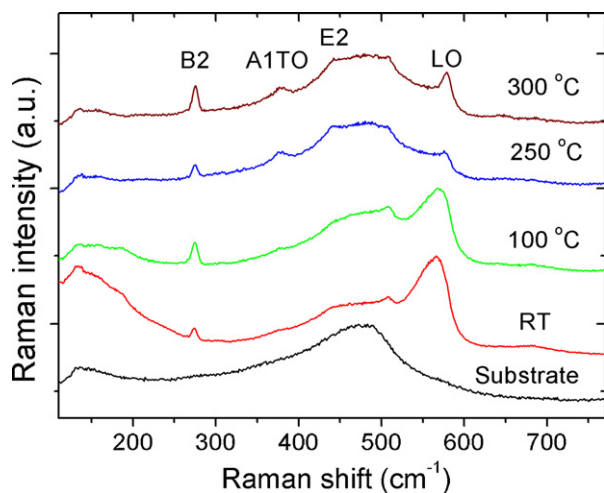


Fig. 4. Normalized Raman spectra taken on the surface of samples A (deposited at RT), B (100°C), C (250°C) and D (300°C). The substrate Raman spectrum is also represented.

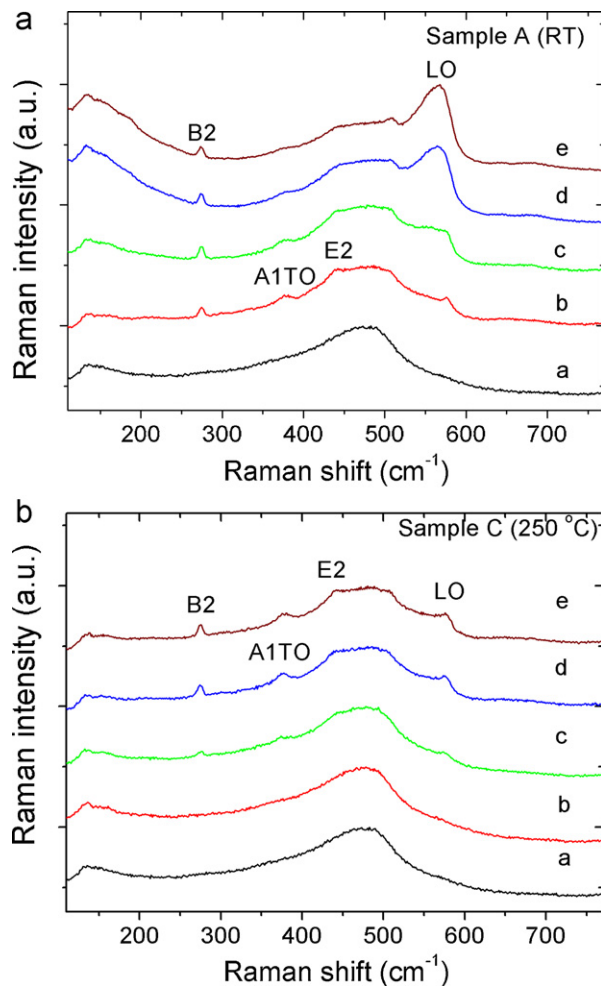


Fig. 5. Normalized Raman spectra taken on samples A and C at the centre of the groove (a), at the groove edge (b), at $4\text{ }\mu\text{m}$ (c) and $8\text{ }\mu\text{m}$ (d) from the groove edge, and at a point on the surface far from the groove (e). The grooves were made at low repetition frequency (20 kHz) and with the sample out of focus. Sample A and sample C were deposited at RT and 250°C , respectively.

In the case of the sample C (Fig. 5b) no substantial differences between the spectra taken at different points were observed. The spectrum taken at the centre of the groove is very similar to the one of the substrate. Over the groove wall (Fig. 5b, spectrum b) the lesser quantity of material leads to less intensity peaks, but they have the characteristics of the surface without attacking. On the other hand, the spectra of the sample deposited at RT (Fig. 5a) showed a clear change. As the measured zone is closer to the groove the wide bands located at $\sim 530\text{--}590\text{ cm}^{-1}$ and $\sim 100\text{--}250\text{ cm}^{-1}$ reduced its size. The $\sim 530\text{--}590\text{ cm}^{-1}$ band also was slightly shifted to the higher energies. The peak located at $\sim 510\text{ cm}^{-1}$ reduces its intensity and a weak peak appears about $\sim 440\text{ cm}^{-1}$, while the peak at 270 cm^{-1} remains invariable.

The changes observed in the spectra of the sample deposited at RT near the groove were due to the influence of the heat transmitted to the material during the laser process. This heat changed the film structure in that zone, becoming similar to the structure of the film deposited at higher temperature. Since the spectra of zones d and e regain the shape of the spectra of films deposited at low temperature we can postulate that the heat affected zone can reach up to $17\text{ }\mu\text{m}$ from the centre of the groove.

4. Conclusions

In the present work a study of the ablation of AZO thin films deposited at different temperature conditions with nanosecond UV laser light for photovoltaic devices has been performed. The ablation threshold of AZO thin films was measured and related with the absorption coefficient of the films at the laser wavelength, showing a direct correspondence.

The set of parameters needed to obtain grooves with good morphological characteristics was explored. An important influence of the rhythm of the flow of energy to the material, especially with the repetition frequency, was observed. At high repetition frequencies the material melted easily, forming ridges of solidified material at the groove edges. Grooves with good morphologic features were obtained working at low repetition frequencies (20 kHz) and with the sample positioned slightly out of the laser beam focus.

Raman spectroscopy was used to study the surface and groove proximities. A change in the material structure in the areas closest to the edges of the laser groove was observed in samples A and B

deposited at RT and $100\text{ }^\circ\text{C}$. In these areas the structure looked like the structure of the films deposited at temperatures over $200\text{ }^\circ\text{C}$. The affected area was quite wide, reaching several microns at each side of the groove. A study of this influence and its relation to thermal and optoelectronic properties of the material will be done.

Acknowledgements

Partial financial support for this work has been provided by the Spanish Ministry of Science and Innovation under the projects AMIC (ENE2010-21384-C04-01) and INNDISOL (IPT-420000-2010-6).

Special thanks must be given to J.D. Santos for the support and discussions about the AZO optical properties during the preparation of this work.

References

- [1] S. Fernández, A. Martínez-Steele, J.J. Gandía, F.B. Naranjo, Radio frequency sputter deposition of high-quality conductive and transparent ZnO: Al films on polymer substrates for thin film solar cells applications, *Thin Solid Films* 517 (2009) 3152–3156.
- [2] A. Buzás, Z. Geretovszky, Patterning ZnO layers with frequency doubled and quadrupled Nd:YAG laser for PV application, *Thin Solid Films* 515 (2007) 8495–8499.
- [3] Q. Qiao, K. Ma, Y.Q. Wang, G.C. Zhang, Z.R. Shi, G.H. Li, Optimization of laser patterning of textured gallium-doped zinc oxide for amorphous silicon photovoltaics, *Appl. Surf. Sci.* 256 (2010) 4656–4660.
- [4] C. Molpeceres, S. Lauzurica, J.J. García-Ballesteros, M. Morales, G. Guadaño, J.L. Ocaña, S. Fernández, J.J. Gandía, F. Villar, O. Nos, J. Bertomeu, Selective ablation of photovoltaic materials with UV laser sources for monolithic interconnection of devices based on a-Si:H, *Mater. Sci. Eng. B* 159–160 (2009) 18–22.
- [5] S.H. Jeong, J.H. Boo, Influence of target-to-substrate distance on the properties of AZO films grown by RF magnetron sputtering, *Thin Solid Films* 447–448 (2004) 105–110.
- [6] E.G. Birgin, I. Chamboleyron, J.M. Martínez, Estimation of optical constants of thin films using unconstrained optimization, *J. Comp. Phys.* 151 (1999) 862–880.
- [7] J.M. Liu, Simple technique for measurements of pulsed Gaussian-beam spot sizes, *Opt. Lett.* 7 (1982) 196–198.
- [8] J. Bonse, J.M. Wrobel, J. Krüger, W. Kautek, Ultrashort-pulse laser ablation of indium phosphide in air, *Appl. Phys. A: Mater. Sci. Process.* 72 (2001) 89–94.
- [9] M. Tzolov, N. Tzenov, D. Dimova-Malinovska, M. Kalitzova, C. Pizzuto, G. Vitali, G. Zollo, I. Ivanov, Vibrational properties and structure of undoped and Al-doped ZnO films deposited by RF magnetron sputtering, *Thin Solid Films* 379 (2000) 28–36.
- [10] F.J. Manjón, B. Marí, J. Serrano, A.H. Romero, Silent Raman modes in zinc oxide and related nitrides, *J. Appl. Phys.* 97 (2005) 053516.